

there is a barrier of >1 eV height to H_2 dissociation. If $CO(a)$ and H_2 approach in suitable geometry, these states have a common symmetry and interact extremely strongly so that the resulting calculated lower *adiabatic* surface¹³ transforms smoothly from $CO(a) + H_2$ to $CO + H + H$ with *no* significant barrier. This result suggests a pathway for this very efficient quenching process. For $N_2(A) + H_2$, however, two different orientations of the reagents yield very different behavior. In a T configuration,¹⁴ with the N_2 approaching the midpoint of the H_2 bond, no mixing of the states occurs (because of differing symmetry) and a barrier of >1.2 eV for access to the $H_2(b) + N_2(X)$ surface is found. In a configuration with the H_2 and N_2 bond axes parallel to each other and approaching in C_{2v} symmetry, symmetry-allowed mixing is observed, and an adiabatic pathway from reagents to products results, but with a barrier of ~ 0.5 eV.

As yet, no dynamical calculations have been carried out, but the considerably lower barrier in the parallel configuration suggests that the quenching process occurs principally by passage over the barrier. As the electronic transitions in CF_3Cl , CF_2HCl , and H_2O are expected to be $\sigma \rightarrow \sigma^*$ or $n \rightarrow \sigma^*$ in the bond $R-X$ to be broken, rather similar behavior may be found for the interactions of these species with $N_2(A)$. Such an analogy would provide an explanation for the low rate constants found for $N_2(A, v=0)$, with the increase in k_v with v due to increased passage over the barrier. It is of interest, however, to attempt to reconcile this model, in which H_2 distortion occurs *before* energy transfer is complete, with the picture of near-vertical transitions in N_2 and RX , as suggested by the correlation of Figure 9. The key is revealed by the calculations: the height of the barrier to cleavage of the $H-H$ bond ($R-X$ in general) is critically dependent on the N_2 bond length, $R(N_2)$. In particular, it is minimized for $R(N_2) \sim 1.19$ Å, approximately midway between the bondlengths of $N_2(A)$ ($R_e = 1.29$ Å) and $N_2(X)$ ($R_e = 1.09$ Å) (which reflects the intimate mixing of the two electronic configurations in this region). This implies that, for optimum passage over the barrier, the N_2 bond must be greatly compressed, and thus for a given $N_2(A, v)$ level,

only a small fraction of collisions, in which N_2 is close to its inner turning point, has the possibility of surmounting the barrier. It is interesting that the empirical correlation leads to the same conclusion; examination of the terms contributing to σ_{eff} , eq 13, shows that even for $v' = 0$, transitions to $v'' = 0$ and 1, at $R(N_2)$ close to $R_e(N_2(X))$, are expected to be dominant. Thus, on both models, severe compression of the N_2 bond is required; moreover, on both models, the probability of achieving this is given by a term that is closely related to the appropriate ($v'v''$) Franck-Condon factor.

The "chemical" model, involving passage over the barrier, is intriguing for a further reason. It is clear that certain trajectories will approach the barrier crest but fail to proceed completely to products. Because of the considerable energy transferred from N_2 vibration into the $H-H$ (or $R-X$) bond, it is possible that the result of such collisions will be $H_2 + N_2(A, v_f)$, with $v_f < v_i$ ($f =$ final, $i =$ initial). Thus the surface properties provide a possible model for vibrational relaxation of $N_2(A)$. In particular, it is possible that the sharp transition, observed previously in $N_2(A) + D_2O$ and CF_2HCl ,⁹ from vibrational relaxation for $v = 1$ to electronic quenching for $v > 1$ by these reagents, can be understood in similar fashion.

In conclusion, it is hoped that this study may help "to bring experimentalists and theorists together and to show that the field of thermal elementary reaction kinetics is alive and well".³⁸

Acknowledgment. We gratefully acknowledge the Air Force Office of Scientific Research, Grant 86-0123 and the Air Force Geophysics Laboratory (J.M.T.), Contract F19628-84-K-0005, for support of this work.

Registry No. N_2 , 7727-37-9; O_2 , 7782-44-7; CF_3Cl , 75-72-9; CF_2HCl , 75-45-6; H_2O , 7732-18-5; D_2O , 7789-20-0; H_2 , 1333-74-0; D_2 , 7782-39-0; CF_4 , 75-73-0; CH_4 , 74-82-8; CF_3H , 75-46-7; $CFCl_3$, 75-69-4; N_2O , 10024-97-2.

(38) Kaufman, F. J. *J. Phys. Chem.* 1979, 83, 1.

High-Temperature Fast-Flow Reactor Kinetics Studies of the Reactions of Al with Cl_2 , Al with HCl, and AlCl with Cl_2 over Wide Temperature Ranges

Donald F. Rogowski,[†] Paul Marshall,[‡] and Arthur Fontijn*

High-Temperature Reaction Kinetics Laboratory, Department of Chemical Engineering, Rensselaer Polytechnic Institute, Troy, New York 12180-3590 (Received: April 12, 1988)

The high-temperature fast-flow reactor (HTFFR) technique has been used to measure rate coefficients for the title reactions under pseudo-first-order conditions. The relative concentrations of the minor reactants (Al species) were monitored by laser-induced fluorescence. The following $k(T)$ expressions in cm^3 molecule⁻¹ s⁻¹ are obtained: $Al + Cl_2 \rightarrow AlCl + Cl$, $k_1(T) = 7.9 \times 10^{-10} \exp(-780K/T)$ between 425 and 875 K; $Al + HCl \rightarrow AlCl + H$, $k_2(T) = 1.5 \times 10^{-10} \exp(-800K/T)$ between 475 and 1275 K; $AlCl + Cl_2 \rightarrow AlCl_2 + Cl$, $k_3(T) = 9.6 \times 10^{-11} \exp(-610K/T)$ between 400 and 1025 K. Confidence limits are given in the text. Indications are obtained that the expressions for $k_1(T)$ and $k_2(T)$ are approximately valid to at least 1300 and 1700 K, respectively. The results are discussed in terms of a harpooning mechanism and a modified form of collision theory, which takes account of long-range attractive potentials and conservation of angular momentum.

Introduction

The temperature dependence of the kinetics of oxidation reactions of metallic free radicals represents a little-studied subject, of great practical importance.¹ Theoretical understanding and predictive ability are far less than for C/H/O/N type reactions,^{2,3} for which a still inadequate, but much larger, experimental data

base is available. We are engaged in providing an extensive set of rate coefficient data for Al species. Earlier results on reactions of Al and AlO with oxygen oxidizers have been summarized.¹ Most recently, measurements on the reactions of AlCl with O_2

(1) Fontijn, A. *Combust. Sci. Technol.* 1986, 50, 151.

(2) Fontijn, A.; Zellner, R. *Reactions of Small Transient Species, Kinetics and Energetics*; Fontijn, A., Clyne, M. A. A., Eds.; Academic: London, 1983; Chapter 1.

(3) Gardiner, W. C., Jr., Ed. *Combustion Chemistry*; Springer-Verlag: New York, 1984.

[†] Present address: Westvaco Research Center, Covington, VA 24426.

[‡] Present address: Department of Chemistry, University of North Texas, Denton, TX 76203-5068.

and CO₂ have been reported.^{4,5} Together these reactions show an interesting variety of $\ln k$ versus T^{-1} relations, including approximately Arrhenius,⁵ zero or small negative activation energies,^{6,7} and concave upward, best approximated by double exponential expressions.^{4,8} Reasonable, if not always conclusive, a posteriori explanations for all these cases can be given.^{1,2,4-8} In the present work, this effort has been extended to include the reactions



Over the present temperature ranges these reactions show, within experimental error, no deviation from linear Arrhenius $\ln k(T)$ versus T^{-1} dependences.

Technique

The basic reactor design and methodology of the high-temperature fast-flow reactor (HTFFR) technique have been discussed,¹⁰ and details of the most recent design modifications have been described.^{4,7,11} The reactor used here consists of a 60-cm-long, 2.2-cm-i.d. vertical mullite reaction tube, surrounded by resistance heating elements, contained in an insulated vacuum housing. It has a usable temperature range from about 400 to 1800 K. Upstream of the reaction zone free Al atoms are vaporized from an Al-wetted tungsten coil at about 1100–1300 K and are entrained in Ar bath gas. This coil can be resistance-heated directly from an independent power supply. For AlCl reactant production a trace of Cl₂, typically <0.005% of the Ar flow, is added to the bath gas. In earlier experiments it has been shown that this AlCl formation takes place, at least in part, from reaction 1 in the gas phase.⁴ Further downstream Cl₂ or HCl is introduced through a movable inlet, situated at 20 or 10 cm upstream from the observation plane. Relative Al and AlCl concentrations at this plane are monitored by laser-induced fluorescence by using a pulsed Lambda Physik EMG 101 excimer/FL 2002 dye/KDP doubling crystal combination, with coumarin 344 dye. Al is pumped and observed on the ⁵S_{1/2}–³P_{1/2} transition at 262.5 nm. For AlCl the 261.4 nm A–X (0,0) transition is similarly used. For effective removal of interference from the hot reactor walls, a 262-nm, 13-nm fwhm filter is placed in front of the EMI 9813 QA photomultiplier tube for all these observations. The gases used are Ar from the liquid (99.998%) and Cl₂ (99.5%) through the bath gas inlet, and 1% Cl₂ (99.5%) in Ar (99.998%) or 5% HCl (99.995%) in He (99.999%) through the oxidant inlet.

Plots of $\ln [\text{Al}]_{\text{rel}}$ or $\ln [\text{AlCl}]_{\text{rel}}$ versus $[\text{Cl}_2]$ or $[\text{HCl}]$ for fixed reaction zone lengths (fixed oxidant inlet positions) yield straight lines with slopes $-kt$, where t is reaction time. k at each experimental condition is determined by a weighted linear regression.^{4,10,12} From this treatment a σ_k associated with each k is found. The uncertainty in temperature is estimated as $\sigma_T = \pm 25$ K.^{4,5} The temperature dependences of the rate coefficients for reactions 1–3 are best described by

$$k(T) = A \exp(-B/T) \quad (4)$$

(4) Rogowski, D. F.; Fontijn, A. *Symp. (Int.) Combust.*, [Proc.] **1988**, 21, 943.

(5) Rogowski, D. F.; Fontijn, A. *Chem. Phys. Lett.* **1986**, 132, 413.

(6) Fontijn, A.; Felder, W.; Houghton, J. J. *Symp. (Int.) Combust.*, [Proc.] **1977**, 16, 871.

(7) Rogowski, D. F.; English, A. J.; Fontijn, A. *J. Phys. Chem.* **1986**, 90, 1688.

(8) Fontijn, A.; Felder, W. *J. Chem. Phys.* **1977**, 67, 1561.

(9) The thermochemical data used are obtained from: Chase, M. W., Jr.; Davies, C. A.; Downey, J. R., Jr.; Frurip, D. J.; McDonald, R. A.; Syverup, A. N. *J. Phys. Chem. Ref. Data* **1985**, 14.

(10) Fontijn, A.; Felder, W. *Reactive Intermediates in the Gas Phase. Generation and Monitoring*; Setser, D. W., Ed.; Academic: New York, 1979; Chapter 2.

(11) Rogowski, D. F. Ph.D. Thesis, Rensselaer Polytechnic Institute, 1988.

(12) Bevington, P. R. *Data Reduction and Error Analysis for the Physical Sciences*; McGraw-Hill: New York, 1969; p 242. Irvin, J. A.; Quickenden, T. I. *J. Chem. Educ.* **1983**, 60, 711.

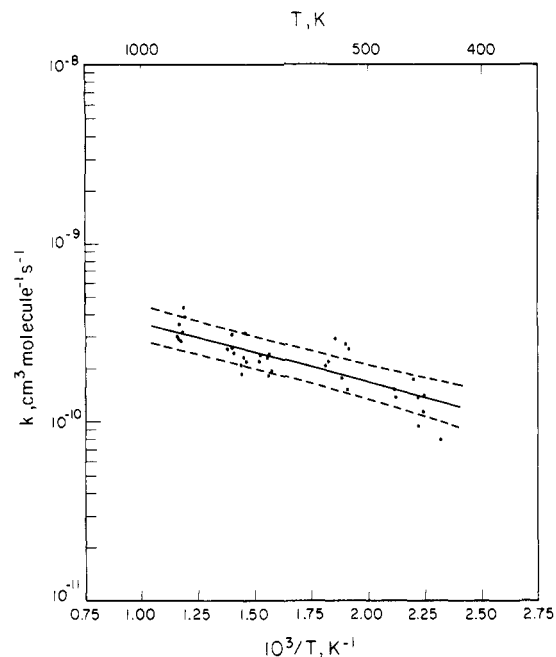


Figure 1. Rate coefficient data for the Al/Cl₂ reaction: (—) rate expression fit of the data given in text; (---) 2 standard deviations to the fit of the rate expression as described in the text.

The parameters for this fit expression are obtained by using regression techniques, which account for σ_k and σ_T .^{11,12} Since A and B are dependent parameters, determination of the uncertainties of the fit requires the covariance σ_{AB} , as well as the variances σ_A^2 and σ_B^2 .¹³ Then, a standard deviation for the fit may be assigned:

$$\sigma_{k(T)} = k(T) [(\sigma_A/A)^2 - 2\sigma_{AB}/AT + (\sigma_B/T)^2 + (0.1)^2]^{1/2} \quad (5)$$

In this expression, the term 0.1 represents σ_η/η , the assigned systematic uncertainty for the flow profile factor η .^{10,14} The resulting $\pm 2\sigma_{k(T)}$ uncertainties are given in the figures showing the data for the individual reactions.

Results

The measured individual rate coefficients for reactions 1–3 and the conditions under which they were obtained are given in Tables I–III, respectively. It may be seen that these rate coefficients are, within the experimental scatter, independent of $[\text{M}]$, the average total concentration, P , the average pressure, \bar{v} , the average gas velocity, and the oxidant inlet to observation plane distance, i.e., the observed reaction zone lengths of 10 or 20 cm.

The 40 rate coefficient measurements for the Al + Cl₂ reaction, (1), between 425 and 875 K give $k_1(T) = 7.85 \times 10^{-10} \times \exp(-779K/T) \text{ cm}^3 \text{ molecule}^{-1} \text{ s}^{-1}$ with associated variances and covariance; cf. eq 4, $\sigma_A^2 = 2.31 \times 10^{-2} A^2$, $\sigma_{AB} = 1.45 \times 10^1 A$, and $\sigma_B^2 = 9.45 \times 10^3$. For the Al + HCl reaction, (2), the 53 measurements from 475 to 1275 K result in $k_2(T) = 1.52 \times 10^{-10} \exp(-803K/T) \text{ cm}^3 \text{ molecule}^{-1} \text{ s}^{-1}$, with $\sigma_A^2 = 1.21 \times 10^{-2} A^2$, $\sigma_{AB} = 8.98 A$, and $\sigma_B^2 = 7.24 \times 10^3$. For the AlCl + Cl₂ reaction, (3), the 60 measurements spanning the 400–1025 K temperature range yield $k_3(T) = 9.56 \times 10^{-11} \exp(-613K/T) \text{ cm}^3 \text{ molecule}^{-1} \text{ s}^{-1}$, with $\sigma_A^2 = 7.38 \times 10^{-3} A^2$, $\sigma_{AB} = 4.49 A$, and $\sigma_B^2 = 3.01 \times 10^3$.

The magnitudes of the rate coefficients obtained at the low pressures used in this investigation indicate that the reactions are bimolecular. The paths given in eq 1–3 represent the only channels accessible from thermochemical considerations.⁹ Reaction 1 was used as the AlCl production reaction for reaction 3 (see the Technique section), and thus the LIF experiments on the latter reaction confirm AlCl as a product species of the former.

A number of additional measurements were made¹¹ on reactions 1 and 2 at temperatures where the Cl₂ and HCl equilibrium

(13) Wentworth, W. E. *J. Chem. Educ.* **1965**, 42, 96.

(14) Fontijn, A.; Felder, W. *J. Phys. Chem.* **1979**, 83, 24.

TABLE I: Summary of Rate Coefficient Measurements of $\text{Al} + \text{Cl}_2 \rightarrow \text{AlCl} + \text{Cl}^a$

oxidant inlet position, cm	\bar{P} , ^b Torr	$[\bar{M}]$, 10^{17} cm^{-3}	$[\text{Cl}_2]$ range, 10^{11} cm^{-3}	\bar{v} , m s^{-1}	\bar{T} , K	k , $10^{-10} \text{ cm}^3 \text{ molecule}^{-1} \text{ s}^{-1}$	$\pm \sigma$, $10^{-10} \text{ cm}^3 \text{ molecule}^{-1} \text{ s}^{-1}$
20	20.2	3.73	3.64–25.1	31	524	1.50	0.10
20	20.2	3.67	3.03–23.8	32	532	1.76	0.14
10	20.3	3.74	3.20–24.4	31	523	2.52	0.18
10	20.3	3.72	2.92–24.8	32	527	2.70	0.21
10	18.2	3.27	2.26–17.6	44	539	2.88	0.24
10	18.3	3.26	2.09–18.4	45	541	2.89	0.24
20	18.3	3.20	2.38–17.4	45	552	2.02	0.15
20	18.3	3.23	2.10–17.0	45	548	2.15	0.15
20	27.1	3.77	3.52–24.8	32	694	2.07	0.13
20	27.1	3.77	3.38–24.3	32	693	1.85	0.16
10	27.1	3.80	3.50–23.4	32	689	2.31	0.17
10	27.1	3.80	3.16–24.6	32	688	3.11	0.19
10	23.0	3.07	2.12–16.6	47	724	2.58	0.24
10	23.1	3.11	2.01–16.9	47	715	3.07	0.19
20	23.1	3.12	2.08–17.7	47	714	2.60	0.19
20	23.1	3.14	2.13–17.0	47	710	2.40	0.19
20	22.2	2.48	1.70–14.3	58	864	2.95	0.16
20	22.3	2.53	1.62–13.8	57	849	2.85	0.17
10	22.3	2.57	1.60–13.6	57	839	4.32	0.38
10	23.1	2.66	1.66–13.8	55	839	3.85	0.27
10	14.9	1.69	1.75–15.3	52	848	3.17	0.30
10	14.9	1.68	1.80–15.0	52	852	3.51	0.35
20	14.9	1.67	2.06–15.1	53	857	2.90	0.24
20	14.9	1.67	1.87–14.9	53	861	3.06	0.26
20	12.3	1.74	2.44–20.0	41	683	2.18	0.21
20	12.3	1.73	2.38–19.7	42	688	2.26	0.21
10	12.3	1.81	2.45–20.3	40	657	2.21	0.24
10	12.4	1.82	2.52–20.2	40	655	2.36	0.26
10	23.1	3.46	2.70–18.6	42	643	2.30	0.18
10	23.1	3.49	2.68–18.5	42	639	2.36	0.22
20	23.1	3.49	2.50–18.9	42	639	1.82	0.13
20	23.1	3.51	2.37–19.9	42	635	1.93	0.14
20	22.9	5.12	3.24–29.8	29	431	0.783	0.06
20	22.9	4.92	3.83–27.2	30	450	0.934	0.10
10	23.0	4.97	3.45–27.2	30	446	1.13	0.10
10	23.0	4.92	2.95–28.4	30	451	1.36	0.12
10	16.4	3.56	2.39–18.4	41	446	1.38	0.12
10	16.5	3.50	2.42–18.0	42	455	1.71	0.21
20	16.5	3.36	2.22–17.9	44	474	1.51	0.12
20	16.5	3.38	2.23–18.8	44	472	1.37	0.11

^aThe measurements are reported in the sequence in which they were obtained. ^b1 Torr = 133.3 Pa.

dissociation exceeds 10%. These data were therefore not used in the above $k(T)$ calculations. However, no significant deviations from the extrapolated $k_1(T)$ were observed until about 1300 K. Further increases in temperature lead to a rapid decrease in k_1 values, indicative of Cl_2 dissociation. The k_2 measurements showed no such dropoff to 1715 K, the highest temperature investigated. It therefore is probable that the $k_1(T)$ and $k_2(T)$ expressions given are applicable at least up to these respective limits.

Discussion

The rate coefficients and the fit expressions are shown in Figures 1–3. Within the scatter of the data, no definite curvature in the Arrhenius plots can be detected. Since the rate coefficients, especially those of reaction 1, are close to gas kinetic, no sharp upward curvature with increasing temperature would have been expected.

There apparently have been no previous experimental measurements of reactions 1–3. However, a theoretical study by Mayer et al., who used a modified BEBO method, predicted $k_1(T) = 2.8 \times 10^{-13} T^{0.67} \exp(-6800K/T)$ and $k_2(T) = 5.5 \times 10^{-13} T^{0.67} \exp(-3900K/T) \text{ cm}^3 \text{ molecule}^{-1} \text{ s}^{-1}$.¹⁵ These values are several orders of magnitude lower than measured here and predict too strong a temperature dependence. While the BEBO approach has led to agreement with experimental data for some H-atom-transfer reactions at 1000 K and above,^{15,16} for reactions involving metal atoms, such as Al, other approaches are needed.

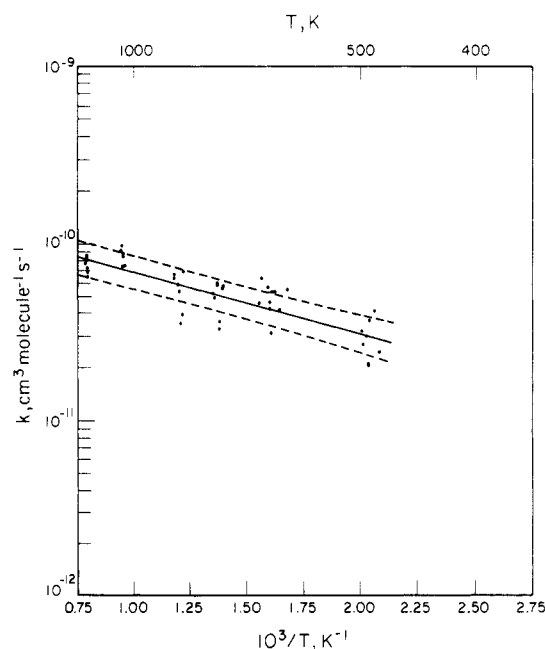


Figure 2. Rate coefficient data for the Al/HCl reaction: (—) rate expression fit of the data given in text; (---) 2 standard deviations to the fit of the rate expression as described in the text.

Al-Atom Reactions 1 and 2. The preexponential factor for reaction 2 is typical for atomic metathesis.^{17a} By contrast reaction

(15) Mayer, S. W.; Schieler, L.; Johnston, H. S. *Symp. (Int.) Combust.*, [Proc.] 1967, 11th, 837.

(16) Mulcahy, M. F. R. *Gas Kinetics*; Nelson: London, 1973; Chapter 5. Zellner, R. In Reference 3, Chapter 3.

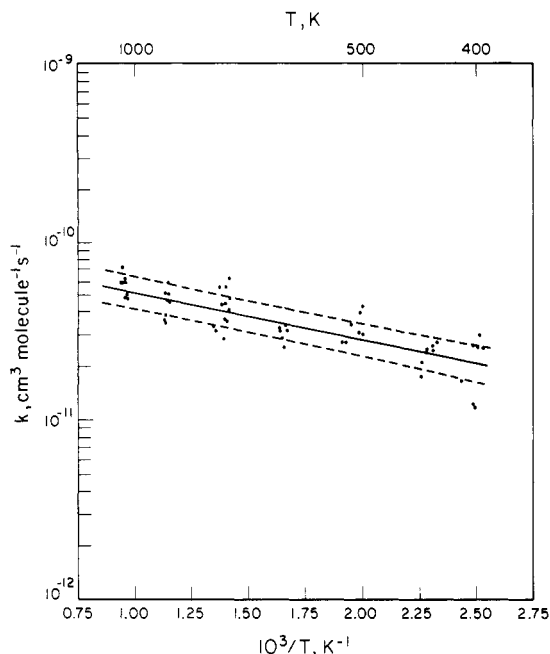


Figure 3. Rate coefficient data for the AlCl/Cl₂ reaction: (—) rate expression fit of the data given in text; (---) 2 standard deviations to the fit of the rate expression as described in the text.

1 has a significantly larger preexponential, which is consistent with an electron-jump mechanism. The simple harpoon model¹⁸ predicts that electron transfer will occur at a separation r_c , where

$$IP(\text{Al}) - EA(\text{Cl}_2) = e^2/4\pi\epsilon_0 r_c \quad (6)$$

Using values for the ionization potential (IP) of Al of 5.986 eV¹⁹ and for the vertical²⁰ electron affinity (EA) of Cl₂ of 1.02 eV,²¹ we calculate a reaction cross section $\sigma = \pi r_c^2$ of 0.26 nm². This is in accord with the mean cross section at the midpoint of the experimental temperature range, $\sigma = 0.28$ nm².

An alternative interpretation of the Al-atom reactions can be based on collision theory. The reaction cross section from simple collision theory in terms of the collision diameter d , the collision energy E_T , and the energy threshold E_0 is²²

$$\begin{aligned} \sigma_{\text{SCT}} &= 0 & E_T < E_0 \\ &= \pi d^2(1 - E_0/E_T) & E_T \geq E_0 \end{aligned} \quad (7)$$

To estimate d we take account of long-range attractive potentials of the form $V(r) = -C_6/r^6$. The maximum impact parameter b_{max} leading to collision is given by²²

$$b_{\text{max}}^2 = (3/2)^{2/3}(3C_6/E_T)^{1/3} \quad (8)$$

Because b_{max}^2 is only weakly dependent on E_T , we shall employ Plane and Saltzman's approximation and set d^2 equal to b_{max}^2 at the mean collision energy of the experiments.²³ Integration of eq 7 over a thermal energy distribution yields the standard result:²²

$$k_{\text{SCT}}(T) = \pi d^2(8k_B T)/\pi\mu^{1/2} \exp(-E_0/RT) \quad (9)$$

For reaction 1 C_6 is estimated via the Slater-Kirkwood expression:²⁴

$$C_6 = 2.48 \times 10^{-78} \alpha_1 \alpha_2 / [(\alpha_1/n_1)^{1/2} + (\alpha_2/n_2)^{1/2}] \text{ J m}^6 \quad (10)$$

(17) Benson, S. W. *Thermochemical Kinetics*, 2nd ed.; Wiley: New York, 1976: (a) p 148; (b) p 157.

(18) Magee, J. L. *J. Chem. Phys.* **1940**, *8*, 687.

(19) Weast, R. C., Astle, M. J., Beyer, W. H., Eds. *CRC Handbook of Chemistry and Physics*, 66th ed.; CRC: Boca Raton, FL, 1985.

(20) Herschbach, D. R. *Adv. Chem. Phys.* **1966**, *10*, 319.

(21) Ayala, J. A.; Wentworth, W. E.; Chen, E. C. M. *J. Phys. Chem.* **1981**, *85*, 768.

(22) Smith, I. W. M. *Kinetics and Dynamics of Elementary Gas Reactions*; Butterworth: London, 1980; Chapter 3.

(23) Plane, J. M. C.; Saltzman, E. S. *J. Chem. Phys.* **1987**, *87*, 4606.

where α_1 and α_2 are the polarization volumes for the reactants expressed in units of 10^{-24} cm³ and n_1 and n_2 are the number of outer-shell electrons. The α values for Al and Cl₂¹⁹ lead to $C_6 = 4.25 \times 10^{-77}$ J m⁶ and hence $\pi d^2 = 0.87$ nm². We fit E_0 to the experimental value of k_1 at 650 K and find $E_0 = 6.1$ kJ mol⁻¹. With this value eq 9 agrees with the experimental fit to $k_1(T)$ to within 15% over the temperature range studied.

We may now apply this simple collision theory to reaction 2. For calculation of C_6 for a system involving dipole-induced dipole forces, these forces are taken into account by an additional term:²⁵

$$C_6 = p^2 \alpha / 4\pi\epsilon_0 \text{ J m}^6 \quad (11)$$

where α is the polarizability volume of Al and p the dipole moment of HCl. Equations 10 and 11 yield contributions to the total C_6 coefficient of 2.48×10^{-77} and 9.7×10^{-79} J m⁶, respectively. The resulting πd^2 is 0.67 nm², which would imply a preexponential factor from eq 9 about 5 times larger than observed for reaction 2. The discrepancy may be due to effects from conservation of angular momentum. González Ureña et al. have shown that among exothermic atom-diatom molecule reactions with low barriers, those that have a ratio of the reduced mass of the products to that of the reactants considerably smaller than 1 may have a reduced cross section and hence a rate coefficient smaller than predicted by eq 9.²⁶ For reaction 2 this ratio is 0.063. This can be contrasted to reaction 1, where this ratio is 1.2 and no angular momentum restrictions arise.²⁶

For the reaction *heavy + heavy-light* → *heavy-heavy + light* the departing light atom carries little angular momentum. Conservation of angular momentum requires therefore that the initial orbital angular momentum of the reactants, which is equal to $(2\mu E_T b^2)^{1/2}$, is almost completely converted to product rotational angular momentum. Here μ is the reduced mass of the reactants and b is the impact parameter. The product angular momentum is $(2I'E'_R)^{1/2}$, where I' is the moment of inertia of the diatomic product and E'_R is its rotational energy.^{26,27} The largest momentum-allowed impact parameter b_{max} is then given by $b_{\text{max}}^2 \approx I'E'_{R,\text{max}}/(\mu E_T)$. The maximum rotational energy $E'_{R,\text{max}}$ reflects the energy disposal of the reaction. Here we shall assume $E'_{R,\text{max}} = \beta(E_T + Q)$, where Q is the reaction exothermicity and β is the fraction of the total available energy that is partitioned into rotation.²³ further assumed to be constant. Noting that $I' \approx \mu r^2$, where r is the equilibrium separation of the heavy-heavy product molecule, i.e., AlCl,²⁷ we can derive a cross section σ_{AM} which is restricted by angular momentum:

$$\sigma_{\text{AM}} = \pi b_{\text{max}}^2 = \pi r^2 \beta (E_T + Q) / E_T \quad (12)$$

σ_{SCT} increases with increasing E_T whereas σ_{AM} decreases, so that the cross section σ reaches a maximum at a collisional energy E_{max} , where

$$E_{\text{max}} = (d^2 E_0 + r^2 \beta Q) / (d^2 - \beta r^2) \quad (13)$$

Thus

$$\begin{aligned} \sigma &= 0 & E_T < E_0 \\ &= \pi d^2(1 - E_0/E_T) & E_0 \leq E_T < E_{\text{max}} \\ &= \pi r^2 \beta(1 + Q/E_T) & E_{\text{max}} \leq E_T \end{aligned} \quad (14)$$

Integrating this σ over a thermal distribution of E_T yields a rate coefficient k_{AM} that reflects the influence of angular momentum conservation:

$$k_{\text{AM}}(T) = k_{\text{SCT}}(T) - \left(\frac{8k_B T}{\pi\mu} \right)^{1/2} \left[\pi d^2 \frac{(RT + E_{\text{max}} - E_0)}{RT} - \pi r^2 \beta \frac{(RT + E_{\text{max}} + Q)}{RT} \right] \exp(-E_{\text{max}}/RT) \quad (15)$$

(24) Pitzer, K. S. *Adv. Chem. Phys.* **1959**, *2*, 59.

(25) Atkins, P. W. *Physical Chemistry*, 2nd ed.; Freeman: New York, 1978; Chapter 23.

(26) González Ureña, A.; Herrero, V. J.; Aoi, F. J. *Chem. Phys.* **1979**, *44*, 81.

(27) González Ureña, A. *Adv. Chem. Phys.* **1987**, *66*, 213.

TABLE II: Summary of Rate Coefficient Measurements of $\text{Al} + \text{HCl} \rightarrow \text{AlCl} + \text{H}^a$

oxidant inlet position, cm	$P,^b$ Torr	$[\bar{M}], 10^{17} \text{ cm}^{-3}$	$[\text{HCl}]$ range, 10^{12} cm^{-3}	$\bar{v}, \text{ m s}^{-1}$	$\bar{T}, \text{ K}$	$k, 10^{-11} \text{ cm}^3 \text{ molecule}^{-1} \text{ s}^{-1}$	$\pm \sigma, 10^{-11} \text{ cm}^3 \text{ molecule}^{-1} \text{ s}^{-1}$
20	12.1	2.43	1.05–9.11	44	481	2.41	0.25
20	12.4	2.39	0.985–8.94	44	499	2.70	0.32
10	12.4	2.46	0.919–8.95	43	486	4.16	0.56
10	12.4	2.43	1.18–8.94	44	492	3.65	0.48
10	20.2	3.90	1.42–10.3	37	500	3.21	0.37
10	20.2	3.94	1.50–11.0	36	495	3.00	0.37
20	20.2	3.97	1.51–10.9	36	492	2.09	0.25
20	20.2	3.97	1.45–10.9	36	492	2.03	0.15
20	30.2	3.48	1.18–9.40	41	836	3.50	0.24
20	30.2	3.50	1.13–9.67	41	832	3.52	0.28
10	30.2	3.53	1.14–9.54	40	827	3.96	0.36
10	30.3	3.55	1.36–9.96	40	822	6.83	0.56
10	16.0	1.86	1.40–10.7	37	833	5.30	0.62
10	16.0	1.84	1.37–10.4	38	841	5.83	0.51
20	16.0	1.82	1.36–9.80	38	850	6.66	0.58
20	16.0	1.81	1.30–10.7	38	849	6.34	0.55
20	20.5	2.67	1.31–9.38	40	742	5.22	0.37
20	20.5	2.68	1.46–9.77	39	739	4.88	0.37
10	20.5	2.71	1.27–9.53	39	732	5.87	0.45
10	20.6	2.71	1.47–9.70	39	731	5.72	0.47
10	28.9	3.86	1.13–9.80	37	722	5.55	0.44
10	28.9	3.88	1.47–10.1	37	718	5.72	0.45
20	28.9	3.83	1.35–10.4	38	729	3.59	0.37
20	28.9	3.83	1.37–10.4	38	729	3.30	0.32
20	25.3	3.92	1.25–11.3	37	623	3.12	0.19
20	25.3	3.91	1.29–11.2	37	625	3.12	0.28
10	25.4	3.91	1.24–9.67	37	627	4.28	0.42
10	25.4	3.92	1.35–10.8	37	626	4.62	0.39
10	18.3	2.80	1.04–7.74	52	630	5.66	0.79
10	18.3	2.75	0.902–7.58	53	642	6.30	0.63
20	18.3	2.73	0.897–7.23	53	646	4.61	0.37
20	18.3	2.74	1.03–7.84	53	644	4.64	0.32
20	15.7	1.43	0.587–4.68	82	1061	9.07	0.91
20	15.7	1.43	0.541–4.71	82	1059	9.75	0.66
10	15.7	1.44	0.487–4.90	82	1053	8.66	0.88
10	15.7	1.44	0.561–5.03	82	1055	9.62	0.87
10	24.6	2.26	0.881–7.05	52	1053	7.24	0.10
10	24.6	2.26	0.851–7.69	52	1053	8.39	0.72
20	24.6	2.27	0.916–7.38	52	1045	7.44	0.71
20	24.6	2.26	1.06–7.09	52	1050	7.41	0.64
20	30.5	2.31	0.920–8.06	51	1275	7.65	0.70
20	30.5	2.32	0.879–7.40	51	1270	8.01	0.58
10	30.5	2.32	0.935–8.43	51	1267	8.54	0.66
10	30.5	2.32	0.937–7.69	51	1265	8.20	0.64
10	40.3	3.08	1.36–10.8	38	1262	7.26	0.58
10	40.3	3.09	1.45–10.1	38	1259	8.04	0.59
20	40.3	3.09	1.41–9.70	38	1257	6.46	0.50
20	40.7	3.11	1.44–9.24	38	1262	6.84	0.46
20	19.6	3.16	1.34–10.9	35	597	5.43	0.37
20	17.8	2.75	0.980–7.82	48	625	5.25	0.41
20	17.9	2.79	1.05–8.11	48	617	5.30	0.40
10	17.8	2.78	0.987–8.35	48	618	5.23	0.58
10	17.8	2.81	0.966–8.19	48	610	4.20	0.48

^aThe measurements are reported in the sequence in which they were obtained. ^b1 Torr = 133.3 Pa.

Qualitatively, it may be seen that if E_{max} is close to E_0 (i.e., β is small) $k_{\text{AM}}(T)$ will have a similar temperature dependence to $k_{\text{SCT}}(T)$ but a smaller preexponential factor.

We have calculated $k_{\text{AM}}(T)$ for the reaction $\text{Al} + \text{HCl}$ using literature values of $Q = 71 \text{ kJ mol}^{-1}$ and $r = 0.213 \text{ nm}^9$ and find agreement to within 5% of the experimental fit expression when $E_0 = 8.3 \text{ kJ mol}^{-1}$ and $\beta = 0.12$. These values correspond to $E_{\text{max}} = 10.4 \text{ kJ mol}^{-1}$. The value of β is consistent with an approximately linear transition state that imparts little torque to the departing AlCl . By contrast, the reaction $\text{Li} + \text{HCl}$ has a larger β of 0.3,^{23,28} an observation that is consistent with the bent transition state derived from ab initio calculations.²⁹ While the particular values of E_0 and β for reaction 2 are best determined by molecular beam techniques, this treatment illustrates that

kinematic effects may have a significant influence on the magnitude of thermal rate coefficients.

AlCl Reaction 3. The measured preexponential of reaction 3, $9.6 \times 10^{-11} \text{ cm}^3 \text{ molecule}^{-1} \text{ s}^{-1}$, is large compared to other metathesis reactions between diatomic reactants.^{17b} This factor, combined with the low activation energy, is consistent with there being a harpooning component to the mechanism: application of the electron-jump model used for reaction 1 with $\text{IP}(\text{AlCl}) = 9.4 \text{ eV}^9$ yields $\sigma = 0.092 \text{ nm}^2$ at 700 K. The experimental value is similar but somewhat smaller, 0.060 nm^2 . We may further view the large preexponential of $k_3(T)$ in terms of the reverse reaction. The equilibrium constant is approximately $2.6 \exp(12700\text{K}/T)$ over the range 400–1000 K,⁹ which implies $k_{-3}(T) \approx 4 \times 10^{-11} \exp(-13300\text{K}/T)$. This preexponential factor is reasonable for an atomic metathesis.^{17a}

General Observations. Reactions 1–3 have large cross sections and are therefore suitable candidates for molecular beam studies, the results of which could permit a more quantitative collision

(28) Becker, C. H.; Casavecchia, P.; Tiedemann, P. W.; Valentini, J. J.; Lee, Y. T. *J. Chem. Phys.* **1980**, *73*, 2833.

(29) Palmieri, P.; Garcia, E.; Laganá, A. *J. Chem. Phys.* **1988**, *88*, 181.

TABLE III: Summary of Rate Coefficient Measurements of $\text{AlCl} + \text{Cl}_2 \rightarrow \text{AlCl}_2 + \text{Cl}^a$

oxidant inlet position, cm	$P, ^b$ Torr	$[\text{M}], 10^{17} \text{ cm}^{-3}$	$[\text{Cl}_2]$ range, 10^{11} cm^{-3}	$\bar{v}, \text{ m s}^{-1}$	$\bar{T}, \text{ K}$	$k, 10^{-11} \text{ cm}^3 \text{ molecule}^{-1} \text{ s}^{-1}$	$\pm\sigma, 10^{-11} \text{ cm}^3 \text{ molecule}^{-1} \text{ s}^{-1}$
20	20.2	4.85	7.34-62.0	26	402	1.23	0.20
20	20.2	4.86	8.44-60.9	26	401	1.17	0.17
10	20.2	4.94	8.75-66.3	26	395	2.57	0.35
10	20.2	4.90	7.79-63.7	26	397	3.01	0.25
10	28.5	6.89	12.1-87.4	19	399	2.56	0.31
10	28.5	6.85	11.4-82.9	19	401	2.66	0.28
20	28.3	6.67	10.5-82.3	19	410	1.66	0.23
20	28.4	6.66	11.3-86.2	19	411	1.17	0.31
10	18.0	3.32	7.58-60.1	27	524	2.74	0.40
10	18.1	3.08	6.57-53.9	29	565	2.09	0.51
20	18.1	2.87	7.05-52.1	32	610	3.17	0.25
20	18.1	2.90	7.32-51.1	31	603	2.57	0.20
20	32.1	5.11	10.6-77.6	21	607	2.91	0.21
20	32.2	5.08	9.82-75.0	21	611	3.28	0.34
10	32.2	5.18	10.9-77.9	20	599	3.15	0.48
10	32.2	5.17	10.1-77.8	20	601	3.40	0.27
20	34.4	4.65	7.28-57.4	27	715	4.49	0.44
20	34.5	4.67	7.86-56.2	27	712	3.63	0.27
10	34.5	4.70	7.55-59.8	27	708	4.16	0.40
10	34.5	4.72	7.39-56.7	27	706	4.81	0.42
10	20.6	2.81	4.61-33.8	45	707	6.17	0.77
10	20.6	2.78	4.79-35.3	46	715	5.59	1.05
20	20.7	2.78	5.43-34.8	46	716	3.70	0.44
20	20.7	2.78	4.91-35.1	46	718	2.84	0.37
20	18.3	2.00	2.93-25.7	64	882	3.66	0.63
20	18.3	2.00	3.00-26.1	64	882	5.15	0.45
20	28.5	3.13	5.44-37.9	41	881	3.88	0.44
20	28.5	3.13	4.72-40.6	41	879	3.48	0.33
10	28.5	3.16	5.37-40.9	41	872	5.96	0.87
10	28.6	3.16	5.14-38.6	41	873	4.70	0.45
10	40.0	4.45	6.76-57.0	29	868	4.59	0.39
10	40.0	4.45	7.25-53.7	29	868	5.10	0.43
20	30.6	2.79	4.30-34.5	46	1061	5.91	0.45
20	30.7	2.83	4.35-34.5	46	1048	5.88	0.53
10	30.6	2.82	4.58-34.1	46	1045	5.95	0.52
10	30.7	2.84	4.25-35.2	46	1042	4.83	0.67
10	42.1	3.85	5.00-43.2	37	1055	7.26	0.71
10	42.3	3.92	5.52-42.4	36	1041	6.22	0.66
20	42.5	3.98	5.54-45.1	36	1031	5.06	0.32
20	42.5	3.99	5.11-44.4	36	1028	4.81	0.36
20	31.2	4.05	6.14-47.2	35	743	3.36	0.35
20	31.3	4.09	5.95-45.8	35	738	3.18	0.35
10	31.3	4.15	5.79-45.7	34	728	5.54	0.61
10	31.3	4.18	5.47-45.7	34	723	4.44	0.56
20	27.4	5.97	10.8-85.7	18	443	1.75	0.14
20	27.5	6.00	12.9-87.5	18	442	2.10	0.26
10	27.5	6.12	13.3-92.1	17	433	2.60	0.29
10	27.5	6.13	12.9-86.7	17	433	2.46	0.30
10	18.4	4.10	8.07-59.7	26	433	2.41	0.58
10	18.4	4.13	8.14-61.0	26	429	2.74	0.36
20	18.4	4.05	8.09-61.5	26	438	2.44	0.30
20	18.4	4.06	8.16-62.1	26	438	2.51	0.21
20	18.3	3.41	6.57-52.6	31	518	2.75	0.24
20	18.3	3.44	6.71-55.2	30	513	3.45	0.47
10	18.3	3.51	7.85-50.7	30	503	4.01	0.52
10	18.3	3.53	6.71-51.5	30	500	4.35	0.56
10	14.8	2.88	7.51-53.2	29	497	2.18	0.58
10	14.9	2.90	7.78-53.5	29	496	3.03	0.69
20	14.9	2.88	7.74-55.4	29	499	3.01	0.26
20	14.9	2.85	7.39-52.9	29	504	3.09	0.26

^aThe measurements are reported in the sequence in which they were obtained. ^b1 Torr = 133.3 Pa.

theory interpretation of reactions 2 and 3. Further theoretical development is also desirable to satisfactorily describe these reactions.

It is interesting to compare $k(T)$ for the $\text{Al} + \text{Cl}_2$ and $\text{Al} + \text{HCl}$ reactions to the $k = 3.4 \times 10^{-11} \text{ cm}^3 \text{ molecule}^{-1} \text{ s}^{-1}$, independent of temperature from 300 to 1700 K, obtained for the $\text{Al} + \text{O}_2$ reaction.⁶ That reaction apparently goes through an intermediate complex, which preferentially dissociates to the original reactants.^{1,2,6} The positive temperature dependence of reactions 1 and 2, as well as their larger preexponentials, indicates that no such complex is formed in these Cl-transfer reactions. Similarly, $k_3(T)$ may be compared to the $k(T)$ of the $\text{AlCl} + \text{O}_2$ and AlCl

+ CO_2 reactions of $1.3 \times 10^{-12} \exp(-3400K/T) + 3.4 \times 10^{-9} \exp(-16100K/T)$ from 490 to 1750 K⁴ and $2.5 \times 10^{-12} \exp(-7550K/T) \text{ cm}^3 \text{ molecule}^{-1} \text{ s}^{-1}$ from 1175 to 1775 K,⁵ respectively. All three reactions have positive temperature dependences, but the Cl-transfer reaction 3 is, in the observed temperature regime, more than 2 orders of magnitude faster than the other two reactions.

Acknowledgment. This work is supported under Grant AFOSR 86-0019, Dr. M. A. Birkan, technical monitor.

Registry No. Al, 7429-90-5; AlCl , 13595-81-8; Cl_2 , 7782-50-5; HCl , 7647-01-0.